NIH Public Access
Author Manuscript
Dev Dyn. Author manuscript; available in PMC 2008 December 3.

Published in final edited form as:
Dev Dyn. 2008 December ; 237(12): 3464–3476. doi:10.1002/dvdy.21598.

Morphogenesis of the node and notochord: the cellular basis for the establishment and maintenance of left-right asymmetry in the mouse

Jeffrey D. Lee and **Kathryn V. Anderson**
Developmental Biology Program, Sloan-Kettering Institute, 1275 York Avenue, New York, NY 10065, USA

Abstract

Establishment of left-right asymmetry in the mouse embryo depends on leftward laminar fluid flow in the node, which initiates a signaling cascade that is confined to the left side of the embryo. Leftward fluid flow depends on two cellular processes: motility of the cilia that generate the flow and morphogenesis of the node, the structure where the cilia reside. Here we provide an overview of the current understanding and unresolved questions about the regulation of ciliary motility and node structure. Analysis of mouse mutants has shown that the motile cilia must have a specific structure and length, and that they must point posteriorly to generate the necessary leftward fluid flow. However, the precise structure of the motile cilia is not clear and the mechanisms that position cilia on node cells have not been defined. The mouse node is a teardrop-shaped pit at the distal tip of the early embryo, but the morphogenetic events that create the mature node from cells derived from the primitive streak are only beginning to be characterized. Recent live imaging experiments support earlier scanning electron microscopy (SEM) studies and show that node assembly is a multi-step process in which clusters of node precursors appear on the embryo surface as overlying endoderm cells are removed. We present additional SEM and confocal microscopy studies that help define the transition stages during node morphogenesis. After the initiation of left-sided signaling, the notochordal plate, which is contiguous with the node, generates a barrier at the embryonic midline that restricts the cascade of gene expression to the left side of the embryo. The field is now poised to dissect the genetic and cellular mechanisms that create and organize the specialized cells of the node and midline that are essential for left-right asymmetry.

Keywords

mouse; embryo; node; notochord; cilia; left-right asymmetry

Introduction

Left-right (LR) asymmetry is a common feature of all vertebrates (Levin, 2005; Raya and Belmonte, 2006). Although left-right asymmetries are not obvious from external appearance, there are pronounced differences between the left and right sides in the structure and placement of internal organs, the organization of the circulatory system and the structure of the brain. In all vertebrate species that have been examined, enhanced left-sided activity of the secreted TGFβ family proteins Nodal and Lefty-2, and the homeobox protein Pitx2, play central roles in the initiation of left-right asymmetry (fig. 1; Shiratori and Hamada, 2006; Schlueter and Brand, 2007). The Nodal, Hedgehog, Fgf, Wnt, Bmp and Notch signaling pathways all converge to regulate the activity of Nodal; these processes have recently been reviewed (Hirokawa et al., 2006; Raya and Belmonte, 2006; Shiratori and Hamada, 2006).

NIH-PA Author Manuscript
NIH-PA Author Manuscript
NIH-PA Author Manuscript

NIH-PA Author Manuscript

NIH-PA Author Manuscript

NIH-PA Author Manuscript

Here we focus on the cell biological processes that are essential to initiate and maintain left-right asymmetry in the mouse embryo. Genetic and embryological experiments in the mouse have shown that asymmetric activation of Nodal also depends on the cellular structure and tissue organization of two midline structures: the node, a morphologically distinct group of cells at the tip of the early mouse embryo, and the axial midline. Motile cilia on the mouse node generate a leftward flow of fluid that is essential to initiate expression of Nodal specifically on the left side of the early somite stage embryo (Hirokawa et. al., 2006). This leftward flow depends on the structure of nodal cilia, their position on node cells and the physical organization of the ciliated cells within the node. Maintenance of left-right asymmetry depends on the organization of the cells of the axial midline, which confine Nodal signals to the left side of the embryo.

Here we discuss the cellular events required for the formation and positioning of the node cilia, two processes that are necessary for the initiation of left-right asymmetry. We go on to provide an overview of previous studies and our own observations on the morphogenetic events that create the node and axial midline with the topology necessary for the initiation and maintenance of left-right patterning.

Ciliogenesis in the mouse node

It is well established that motile cilia are essential for left-right asymmetry (Hagiwara et al., 2004; Bisgrove and Yost, 2006; Hirokawa et al., 2006; Satir and Christensen, 2007). Long before it was known that the mouse node was the source of left-right asymmetry, it was recognized that each cell of the ventral node has a single cilium projecting from its apical (outward facing) surface (Jurand, 1974). Mutant mouse embryos that completely lack cilia show abnormal left-right patterning, which can first be recognized morphologically as randomized polarity of heart looping and molecularly by the bilateral expression of *nodal* in the lateral plate mesoderm (Nonaka et al., 1998; Takeda et al., 1999; Murcia et al., 2000; Huangfu et al., 2003). Similarly, mouse mutants in which node cilia are present but not motile show the same type of disruption of left-right asymmetry (McGrath et al., 2003).

Using live imaging and embryological manipulations, several groups demonstrated that mouse node cilia are motile and that they produce a leftward flow of extracellular fluid ("nodal flow"). Further experimental manipulations demonstrated that leftward flow of fluid across the node is both necessary and sufficient to establish LR asymmetry (Nonaka et al., 1998; Okada et al., 1999; Supp et al., 1999; Takeda et al., 1999; Nonaka et al., 2002). Nodal flow is required during a short time window, from the 1–6 somite stage, which spans 6–7 hours of development (Shiratori and Hamada, 2006).

Cilia formation

Cilia are built around a ring of nine doublet microtubules that extend the length of the cilium. Formation of cilia depends on a common core machinery, including a specific kinesin-2 motor that carries cargo to the tip of the cilium, intraflagellar transport (IFT) particles, and a retrograde cytoplasmic dynein motor (Hagiwara et al., 2004). Mouse node cilia are relatively long: at embryonic day 7.5 (e7.5), or LS/0B (late streak/zero bud) stage (for staging nomenclature, see Downs and Davies, 1993), they are ~1.5 microns long and they grow to about 3–5 microns in length by EHF (~e8.0) stage (fig. 2A; Sulik et al., 1994).

Several transcription factors are required for the formation of normal node cilia. Foxj1 is specifically required for the formation of motile cilia in tissues such as the lung (Chen et al., 1998). In the absence of Foxj1, cilia of normal length are present on the node but appear to be immotile, and situs is randomized as a result (Chen et al., 1998; Brody et al., 2000; Zhang et al., 2004). Rfx3 is one of five mammalian homologues of *C. elegans daf-19* (Emery et al.,

NIH-PA Author Manuscript

NIH-PA Author Manuscript

NIH-PA Author Manuscript

1996). The *daf-19* transcription factor binds to X-box motifs which are present in the regulatory regions of many cilia genes; *daf-19* is required for the transcription of cilia genes in *C. elegans* (Swoboda et al., 2000). While *Rfx3* mutants do form nodal cilia, the cilia grow slowly and are only half the length of wild-type cilia at the 2-somite stage, when nodal flow is required (Bonnafe et al., 2004). *Rfx3* mutants show randomized LR situs (Bonnafe et al., 2004), suggesting that cilia must have a specific length, presumably in order to generate effective nodal flow. Nodal cilia in embryos lacking the homeobox transcription factor Noto are short and have abnormal microtubule axonemes, and the mutant embryos have randomized situs (Beckers et al., 2007). Expression of both *Foxj1* and *Rfx3* is decreased in the node of *Noto* mutants (Beckers et al., 2007), suggesting that Noto acts upstream of Foxj1 and Rfx3 in a transcriptional pathway that regulates morphogenesis of node cilia.

Cilia motility

The first connection between ciliary motility and LR patterning came from studies of the classic mouse recessive mutation *inversus viscerum (iv)*; *iv/iv* mice have randomized LR asymmetry (Hummel and Chapman, 1959; Layton, 1976). The *iv* gene encodes Left-right dynein (Lrd; MGI: Dnahc11), an axonemal dynein motor protein that is required for the motility of node cilia (McGrath et al., 2003). Approximately 70% of the node cilia are motile and express Lrd (McGrath et al., 2003). The remaining node cilia do not express Lrd and are presumably immotile. The two types of cilia are interspersed, and it is not known if the two classes of cilia are arranged in a stereotyped pattern.

The precise structure of the motile cilia in the mouse node is still a point of discussion. Motile cilia, such as those of the respiratory tract or oviduct, generally have nine outer doublets and a single pair of central microtubules (9+2 configuration) in the ciliary axoneme; motion in these cilia is produced by the inner and outer dynein arms, which cause the central microtubules to slide past one another (Davenport and Yoder, 2005; Satir and Christensen, 2007). In contrast, primary cilia, so called because they are typically found as a single cilium per cell, generally have a 9+0 microtubule arrangement, i.e. they lack the central microtubule pair. 9+0 cilia are usually thought to be immotile. Transmission EM of node cilia showed a 9+0 microtubule organization with dynein arms that connect neighboring microtubule doublets (Sulik et al., 1994; Takeda et al., 1999; Essner et al., 2002). Remarkably, node cilia produce a vortical motion in which the cilium maintains a straight extended orientation but the distal end moves in a circle around the axis of rotation, in contrast to the whip-like back-and-forth motion characteristic of 9+2 cilia (Nonaka et al., 1998); this suggests that 9+0 cilia use a novel mechanism for motility. However, two recent studies have identified 9+2 cilia in the mouse node and 9+2 and 9+4 cilia in the rabbit posterior notochordal plate (PNC; the structure that generates leftward flow in the rabbit embryo), perhaps due to improved fixation conditions (Feistel and Blum, 2006; Caspary et al., 2007). Thus additional studies are needed to define the structure and spatial organization of motile cilia.

The mechanism by which nodal flow is translated into asymmetric expression of *nodal* is still an area of active research. Two primary models have been proposed, known as the morphogen and the two-cilia models. The morphogen model proposes that nodal flow produces a gradient of a signaling molecule in the node (Nonaka et al., 1998; Okada et al., 2005), while the two-cilia model proposes that nodal flow causes the deformation of mechanosensory cilia on the left side of the node (Brueckner, 2001; Tabin and Vogan, 2003). In either case, nodal flow appears to be linked to an increased influx of Ca^{++} ions on the left periphery of the node. This asymmetric Ca^{++} influx is linked to the asymmetric activation of *nodal* expression in the left LPM (McGrath et al., 2003; Tanaka et al., 2005). Mutation of the *Polycystin-2 (Pkd2)* gene, which encodes a protein that is likely to be a Ca^{++} channel, blocks elevated Ca^{++} and randomizes the LR axis (Pennekamp et al., 2002; McGrath et al., 2003). The morphogen and

NIH-PA Author Manuscript

NIH-PA Author Manuscript

NIH-PA Author Manuscript

two-cilia models are discussed in depth in several excellent recent reviews (Levin, 2005; Hirokawa et al., 2006; Raya and Belmonte, 2006; Shiratori and Hamada, 2006).

Cilia position

In addition to cilia structure and motility, normal nodal flow appears to depend on the precise position of cilia on node cells. The vortical rotation of nodal cilia would seem to preclude the generation of a laminar leftward flow, but hydrodynamic modeling predicted that that rotating cilia could produce a leftward flow if the axis of rotation were pointed towards the posterior of the node, which would produce a more effective stroke towards the left side of the node (Cartwright et al., 2004). Direct observation confirmed that cilia are indeed positioned toward the posterior of each node cell (Nonaka et al., 2005; Okada et al., 2005). The surface of each central node cell is domed (Okada et. al., 2005); when the posteriorly positioned cilium exits perpendicular to the surface, it is angled 25–40° towards the posterior. Thus, the function of nodal cilia as producers of leftward flow depends both on cilia motility and the posterior tilt of each cilium, which in turn relies on the curved apical surface of each pit cell and the posterior emergence point of each cilium. Apical doming is not a general characteristic of columnar epithelia. This suggests that doming of cells in the node pit is actively regulated; however, the mechanism of this regulation is unknown.

The importance of cilia orientation is supported by the analysis of *inversin (inv)* mutant mice (Okada et al., 2005). The *inv* mutation, which is caused by a transgene insertion, is unusual because it causes a reversal of left-right asymmetry rather than randomization or isomerization of the axes (Yokoyama et al., 1993). Nodal flow in *inv* mutants is slow and not polarized, and 20% of the cilia in the mutant are pointed anteriorly rather than posteriorly (Okada et al., 2005). The misorientation of cilia may be due to defects in mechanisms that position cilia or could be due to the disruption of node structure in the mutants (Okada et al., 1999).

The coordinated polarization of cilia position across the epithelium of the ventral node is a type of planar polarity, in which cells in an epithelium produce polarized structures or undergo polarized movements in the plane of the epithelial sheet (Okada et al., 2005; Bisgrove and Yost, 2006; Wang and Nathans, 2007). In this case, the cilium in each cell of the mature node is positioned towards the posterior of the cell within the plane of the ventral node. In the neural plate and inner ear, genes of the non-canonical Wnt/planar cell polarity pathway control planar polarity (Wang and Nathans, 2007). However, mutants in the mouse non-canonical Wnt pathway, including *Vangl2, Celsr1, Scrib, Fz3/6* double mutants and *Dvl1/2* double mutants, do not have obvious defects in the polarity of heart looping or other aspects of left-right asymmetry (Hamblet et al., 2002; Curtin et al., 2003; Montcouquiol et al., 2003; Murdoch et al., 2003; Torban et al., 2004; Wang et al., 2006). Thus the signals that control cilia position remain undefined.

In the posterior notochordal plate of the rabbit embryo and in the gastrocoel roof plate of the *Xenopus* embryo (the tissues that generate leftward flow), cilia are initially located in the center of the apical surface of each cell, but later become posteriorly localized (Feistel and Blum, 2006; Schweickert et al., 2007). We have made similar observations in the mouse node: at the LS/0B stage (~e7.25) most nodal cilia are located in the center of the cell, but they become posteriorly biased at later stages (unpublished and Fig. 6A; schematized in Fig. 2B, C). At the EHF stage (~e7.75), the basal bodies from which cilia emerge are also posteriorly localized (Nonaka et al., 2005); basal body position at intermediate stages of node formation has not been examined. The repositioning of node cilia is reminiscent of events that occur during establishment of planar polarity in the inner ear (Kelly and Chen, 2007). The kinocilium (the primary cilium of cochlear hair cells) is localized to the posterior of each hair cell in the cochlea, where it organizes a chevron-shaped arrangement of actin-based stereocilia around it. However, the kinocilium initially forms in the middle of the cell; it later moves away from the

NIH-PA Author Manuscript

NIH-PA Author Manuscript

NIH-PA Author Manuscript

midline along the mediolateral axis (Sobkowicz et al., 1995; Frolenkov et al., 2004; Jones et al., 2008). Thus it is possible that the posterior position of nodal cilia depends on regulated movement of the basal body to the posterior of the cell.

Morphogenesis of the mouse node

Anatomy of the mouse node and the organs of asymmetry in other vertebrate embryos

The cilia that generate the leftward fluid flow in the mouse embryo are localized to the node, a specialized group of cells at the distal tip of the early embryo. Anatomical comparisons between vertebrate species and current models of nodal flow suggest that a smooth, ciliated surface over which laminar fluid flow moves leftward, is important for LR patterning (Hirokawa et al., 2006).

In the mouse, the leftward flow generated by ciliary motility in the node begins at LB/EHF (~e7.5) stages (Nonaka et al., 1998). The mature node of the EHF stage (~e7.75) embryo is visible by scanning electron microscopy (SEM) as a concave, teardrop-shaped epithelial field of cells located distally on the ventral surface of the embryo (Fig. 3A). The mature node is composed of approximately 250 cells in a pit approximately 50–60 μm wide, 70–90 μm long and up to 50 μm deep (Sulik et al., 1994; Yamanaka et al., 2007). The node is composed of two columnar epithelial layers with apposed basal surfaces: the dorsal node is contiguous with the surrounding epiblast, whereas the ventral node is contiguous with adjacent endodermal epithelium (Fig. 3 A, C). The cells in the node pit and notochordal plate, which extends anteriorly from the node, display apical-basal polarity and characteristically have small apical (outer) surfaces, as visualized by either SEM (Sulik et al., 1994) or confocal microscopy (Fig. 3B, Fig 8B). The cells of both the node pit and the notochordal plate are also characterized by a prominent monocilium on their apical surfaces (Jurand, 1974; Poelmann, 1981; Sulik et al., 1994). The node pit is surrounded by 20–30 squamous cells with larger apical surfaces, called crown cells, that are contiguous with the surrounding endoderm (Fig. 3A, Fig 5E).

There are interesting interspecific variations in the structure of the tissues that produce and receive the leftward flow (schematized in Fig. 4). The mouse node is covered on its ventral surface by Reichardt's membrane, which produces a small, contained space for nodal flow (Fig. 4A). The posterior notochordal plate (PNC) is the ciliated structure that produces leftward flow in the rabbit embryo (Okada et al., 2005). The PNC is wider than the trunk notochordal plate (Feistel and Blum, 2006;Blum et al., 2007) and forms a more elongated structure than the shorter triangle shape of the mouse node. Unlike the mouse ventral node, the ventral surface of the rabbit PNC is convex, curving out towards the ventral surface (Okada et al., 2005;Blum et al., 2007). In the rabbit PNC the rightward “return” flow travels along the posterior margin of the PNC, whereas in the mouse node the return flow travels directly across the node, in a layer more removed from the node surface than the leftward flow (Okada et al., 2005). It is possible that this difference in fluid movement may be due to the differences in shape between these organs.

Kupffer’s vesicle (KV) is a transient spherical structure that forms in the tailbud of teleost fish embryos near the end of gastrulation (Essner et al., 2002). Each cell in the zebrafish KV epithelium projects a single 9+2 monocilium into the lumen of the vesicle (Cooper and D'Amico, 1996; Melby et al., 1996; Kramer-Zucker et al., 2005; Amack et al., 2007). These cilia tilt towards the posterior and they rotate vortically, like mouse node cilia (Essner et al., 2005; Kramer-Zucker et al., 2005). Recent 3D image analysis addressed a puzzling aspect of KV geometry: how cilia projecting into a spherical vesicle could produce a net leftward flow of fluid. This analysis demonstrated that 80% of the KV cilia are in the dorsal hemisphere, and those cilia are enriched in the anterior third of the dorsal side (Kreiling et al., 2007). The dorsal enrichment of cilia is topologically similar to the mouse node and may account for net leftward

NIH-PA Author Manuscript

NIH-PA Author Manuscript

NIH-PA Author Manuscript

flow. In the medakafish, only the dorsal surface of the KV is ciliated; this surface is convex, and, like the rabbit, the return rightward flow occurs across the posterior side (Okada et al., 2005).

Cilia of the gastrocoel roof plate (GRP) of *Xenopus laevis* also generate a leftward flow. The GRP is very different in structure from the mouse node: it is part of a layer of mesoderm that lies beneath the notochord of the frog gastrula (Shook et al., 2004). GRP cells possess motile monocilia that, like mouse node cilia, project from the posterior of the cell and produce a leftward flow of fluid (Essner et al., 2002; Shook et al., 2004; Okada et al., 2005; Schweickert et al., 2007). No measurement of a return flow was reported in *Xenopus* embryos (Schweickert et al., 2007). It is interesting to note that the GRP does not sit in a recessed pocket of the gastrocoel but rather is flush with the neighboring lateral endoderm (Shook et al., 2004); this suggests that, at least in *Xenopus*, a morphological "wall" is not necessary for the reception of the flow-generated signal. This type of variation between the structures of the organs of asymmetry may reflect differences in how the flow-generated signal is detected (Raya and Belmonte, 2006).

Assembly of the node

Electron microscopy and cell lineage studies have helped define how the stereotyped structure of the mouse node develops (Poelmann 1981; Sulik et al. 1994; Yamanaka et al. 2007). The node arises from a group of cells located near the anterior end of the primitive streak at the mid-streak to late streak (MS to LS) stages. We find that at MS stage the node is not visible and the outer surface of the embryo is covered by squamous endoderm cells (Fig. 5A, B). Morphogenesis of the mouse node begins when several groups of columnar cells with small apical surfaces become visible near the distal tip of the embryo at LS (~e7.5) stage (fig. 5C, D; Sulik et al., 1994). Clusters of cells with small apical surfaces are also present more anteriorly on the embryonic midline (fig. 5C; Poelmann, 1981; Sulik et al., 1994). These clusters of cells with small apical surfaces are separated by squamous cells with larger surfaces (Sulik et al., 1994).

At OB stage (e7.5–7.75), the node appears as a single field of cells with small apical surfaces (Fig.5 E, F). At this stage the cilia are approximately 2 μm long and often appear to extend vertically from the surface of the node (Fig. 5F). The node region is flat and set slightly below the neighboring crown cells (Fig. 5E). By EHF stage (~e7.75) the pit of the node has formed and the final shape of the node is established (Fig. 5G). The cilia are 3–4 μm long and project towards the posterior (Fig. 5H).

The transition between these two configurations - multiple small fields of constricted cells separated by endoderm cells and a single field of ventral node cells (Fig. 5C, G) – is only beginning to be described. In 1981, Poelmann proposed that clusters of streak-derived precursors of the node inserted between cells of the endoderm layer (Poelmann, 1981). Recent live imaging experiments have documented the rearrangements of the node cells by following the expression of eGFP knocked into the *noto* locus (Yamanaka et al., 2007). Mouse *noto*, the homologue of *Xenopus Xnot* and zebrafish *floating head*, is expressed exclusively in the node and notochord, and the *Noto-GFP* allele recapitulates this pattern (Abdelkhalek et al., 2004). Before the node is visible on the ventral surface of the embryo, Noto-GFP+ cells are already arranged in a sheet beneath the endodermal layer (Yamanaka et al., 2007). Similarly, ciliated cells have been observed in the rabbit posterior notochord (PNC) at the time of the emergence of the PNC through the overlying hypoblast layer (Feistel and Blum, 2006; Blum et al., 2007). We have detected ciliated cells beneath endoderm of the LS stage (e7.5) mouse embryo by both SEM and confocal microscopy (Fig. 6B, C). Thus the initial patchy appearance of ciliated, columnar cells may reflect the gradual removal of overlying endoderm cells, either by cell death or movement, although the organization of the node precursor cells prior to their

NIH-PA Author Manuscript

NIH-PA Author Manuscript

NIH-PA Author Manuscript

complete emergence is unknown. Node precursors may be present in a single field or several clusters, and it is not known whether the field of node precursors changes shape as the mature node forms. These observations suggest that the behavior of the ventral node and the endoderm are somehow coordinated, so that the endoderm cells migrate off of the presumptive ventral node, at the same time that the ventral node cells converge toward the midline and assemble into the teardrop-shaped pit (summarized in Fig. 7). Nothing is known about how signals between these two tissue layers might coordinate these behaviors.

The ventral node cells must also organize into a columnar epithelium, with its apical surface facing ventrally (the opposite of the epiblast). Noto-GFP+ cells are found in the anterior primitive streak prior to node formation (Yamanaka et al., 2007), which suggests that these cells begin to express Noto and adopt a node or trunk notochord fate as they begin to delaminate from the streak. Presumably the Noto-expressing precursors of the node become mesenchymal as they exit from the primitive streak, but then reform an epithelium (with the opposite polarity as the epiblast) beneath the endodermal layer, before the endoderm cells move away to reveal the node. Ultimately the node epithelium becomes contiguous with the adjacent epithelium of the definitive endoderm. The mechanisms that regulate epithelialization of the ventral node and insertion into the endoderm are not known.

Genetic regulation of node morphogenesis

Specification of the node depends on a transcriptional cascade. The winged-helix transcription factor FoxH1 mediates Nodal signaling during gastrulation; *foxH1* mutants do not form the anterior primitive streak, including the node (Yamamoto et al., 2001). Many other transcription factors are expressed at the distal tip of the embryo before and during node morphogenesis. The T-box gene *T*, the Lim homeodomain gene *Lhx1*, the winged-helix gene *FoxA2*, and the homeodomain protein *Otx2* are all expressed in the node and are required for normal specification of the node (Ang and Rossant, 1994; Rashbass et al., 1994; Shawlot and Behringer, 1995; Ang et al., 1996; Liu et al., 1999). Similarly, *no tail*, the homolog of *T*, is expressed in the zebrafish KV, along with the related *Tbx16* gene (Amack and Yost, 2004). KV formation is blocked at successive stages by mutations in *no tail* and *Tbx16* (Amack et al., 2007). The *noto* gene encodes a homeobox transcription factor that is expressed in the mouse node (Abdelkhalek et al., 2004; Beckers et al., 2007). *noto* mutants have LR patterning defects and display abnormal node morphology: large unciliated cells and smaller ciliated cells are mixed together on the distal surface of the embryo (Beckers et al., 2007). Consistent with this morphological defect, markers of the crown cells such as *nodal* and the Cerberus-like molecule *dante*, are interspersed with cells that express markers of the node pit, like dynein subunits and Noto itself (Beckers et al., 2007). These results suggest that the endoderm cells fail to move in *noto* mutant embryos, and that the pit either does not form or remains partially covered by endoderm.

The Notch pathway appears to play a role in node morphogenesis. Mutations in the Notch ligand *Delta-like1 (Dll1)*, the nuclear transactivator *RBPJ*, and the chromatin-remodeling protein *Baf60c* all partially disrupt the organization of the node (Krebs et al., 2003; Przemeck et al., 2003; Takeuchi et al., 2007). In these mutant embryos, as in *noto* mutants, large endoderm cells are found in the central region of the node. Perinodal expression of *nodal* is lost in *Dll1* mutants, consistent with the presence of RBPJ consensus binding sites in the perinodal enhancer of *nodal* (Krebs et al., 2003; Przemeck et al., 2003; Raya et al., 2003). However, node shape is not affected by mutations in *nodal* that prevent its expression around the node (Brennan et al., 2002). This suggests that Notch signaling may regulate the morphogenetic events that segregate endoderm and ventral node cells in coordination with the regulation of *nodal* expression.

NIH-PA Author Manuscript

NIH-PA Author Manuscript

NIH-PA Author Manuscript

The midline barrier: Morphogenesis of the notochord

Work from many labs has shown that correct initiation of LR asymmetry is not enough to ensure consistent LR patterning; additional mechanisms are required to maintain the fidelity of LR asymmetry. Embryological studies in *Xenopus* and zebrafish have shown that the axial midline is necessary for the maintenance of LR asymmetry (Danos and Yost, 1996; Lohr et al., 1997; Kelly et al., 2002).

The importance of the midline received a molecular underpinning with the discovery that Lefty-1, a TGFβ-related antagonist of Nodal, is expressed in the left side of the floor plate (the ventral midline of the neural tube) and is required for the restriction of left-sided genes to the left LPM (Meno et al., 1996; Meno et al., 1998). Expression of floor plate *lefty-1* is induced by Nodal from the left lateral plate mesoderm, and Lefty1 made in the floor plate prevents diffusing Nodal from triggering the left-side cascade of gene expression in the right lateral plate mesoderm (Yamamoto et al., 2003). Thus the formation and function of the floor plate is critical for the maintenance of LR asymmetry. The presence of the floor plate depends on the notochord, which produces Sonic hedgehog and thereby induces the floor plate (Placzek et al., 1990; Roelink et al., 1994).

In addition to its role in the initiation of LR asymmetry, the node produces the trunk notochord (Beddington, 1994; Sulik et al., 1994; Kinder et al., 2001; Yamanaka et al., 2007). Thus the node and its derivatives are required both to establish and to maintain LR asymmetry. The cells of the axial mesoderm have different origins, depending on their position along the mouse anterior-posterior axis (Fig. 8A). The most anterior axial mesoderm of the mouse, the prechordal plate, is produced from the early gastrula organizer (EGO) shortly after the initiation of gastrulation (Kinder et al., 2001). The anterior notochord, also called the anterior head process, arises slightly later (MS stage, e7.25), from the midgastrula organizer (MGO), and the trunk notochord derives from the cells of the node (Kinder et al., 2001).

As with the node, interesting differences in notochord formation exist between vertebrate species. Notochord in the chick is produced by Hensen's node and to a lesser extent by cells of the anterior primitive streak that migrate through the node (Selleck and Stern, 1991; Psychoyos and Stern, 1996). The rabbit notochord is contiguous with the node; while cell-labeling experiments have not been performed in rabbit, it seems likely that the notochord arises from the node and anterior primitive streak in this species as well (Blum et al., 2007). In contrast, in zebrafish and *Xenopus*, notochord production appears to be independent of Kupffer's vesicle and the gastrocoel roof plate, respectively. The GRP eventually inserts into the overlying notochord (Shook et al., 2004). KV is produced by the dorsal forerunner cells, a group of non-involuting cells at the leading edge of the embryonic shield, which also produces notochord (Cooper and D'Amico, 1996; Melby et al., 1996). Thus while the notochord and KV may have a common origin (the shield), KV does not contribute to the notochord.

At early somite stages (until e9.0) the notochordal plate is a flat epithelial sheet that extends along the ventral midline between the node and the prechordal plate (visible in fig. 8B; Sulik et al., 1994). Each cell of the notochordal plate has a small apical surface and an apical monocilium with the same 9+0 microtubule organization as nodal cilia (Sulik et al., 1994). Despite having a similar structure, cilia of the notochordal plate are reported to be immotile (Okada et al., 2005). During headfold and early somite stages, cells of the notochordal plate converge towards the midline, in a planar cell polarity-dependent process (fig. 8C–E;Ybot-Gonzalez et al., 2007). The notochordal plate then reorganizes to form a solid rod that pinches off from the adjacent gut endoderm and comes to lie beneath the endoderm (Jurand, 1974). The cellular details of the transition from a sheet to a rod have not been characterized.

NIH-PA Author Manuscript

NIH-PA Author Manuscript

NIH-PA Author Manuscript

Fate mapping experiments demonstrated that the trunk notochord is derived from the node (Beddington, 1994; Yamanaka et al., 2007). The ventral node is largely quiescent, as measured by bromodeoxyuridine uptake, beginning at LS/OB stages, when the ventral node first becomes apparent on the outer surface of the embryo, and continuing to 5–7 somite stages (Bellomo et al., 1996). The same study concluded that the notochordal plate is also quiescent at these stages (Bellomo et al., 1996), suggesting that its elongation is due largely to convergent extension, consistent with later studies (Yamanaka et al., 2007; Ybot-Gonzalez et al., 2007). There is also a constant repopulation of the node, as cells from the anterior primitive streak are recruited into the node, presumably to replace cells that moved anteriorly to become notochord (Kinder et al., 2001).

Genetic regulation of the axial midline

Genetic studies have confirmed the regional heterogeneity of the axial mesoderm indicated by the fate-mapping experiments. *FoxA2* mutants do not form node, notochord or prechordal plate (Ang and Rossant, 1994; Weinstein et al., 1994). *T* mutants lack the notochord posterior to somite 7 (Rashbass et al., 1994). *Noto* mutants have only mild abnormalities of tail notochord, but *Noto* mutants that lack one copy of *Foxa2* do not form trunk notochord (Abdelkhalek et al., 2004; Yamanaka et al., 2007). These data are consistent with a genetic hierarchy in which FoxA2 regulates *T* and *Noto* in the notochord (Ang and Rossant, 1994; Weinstein et al., 1994; Abdelkhalek et al., 2004). *Noto* may act primarily to maintain notochord identity; in *Noto* mutants, Noto-GFP+ cells populate the somites, suggesting a switch in fate to paraxial mesoderm (Yamanaka et al., 2007).

Notch signaling also appears to be important for midline specification or maintenance. *Dll1* mutants lack T expression in the notochord (Przemeck et al., 2003). *Dll1* mutants also lack expression of *lefty1* in the midline, perhaps as a result of failure to induce floor plate (Przemeck et al., 2003). It is unknown whether this phenotype is related to the disruption of node shape that occurs earlier in *Dll1* mutants (Przemeck et al., 2003); this possibility needs to be explored further.

The nature of the midline barrier is only partially understood. *lefty1* is expressed in the left prospective floor plate, apparently under the control of Nodal emanating from the left lateral plate mesoderm (Meno et al., 1996; Yamamoto et al., 2003). It is not clear how Lefty1, which is induced by Nodal, could act swiftly enough to inhibit Nodal before it induces Nodal expression in the right LPM. Nor is it clear how *lefty1* expression can be precisely limited to the left half of the prospective floor plate. It is tempting to speculate that some physical barrier transiently impedes Nodal diffusion past the midline until *lefty1* expression is initiated.

The notochord may play more than one role in the establishment of the midline barrier. The floor plate, the site of *lefty1* expression, is induced by Sonic hedgehog (Shh) made by the notochord: *Shh* mutant embryos lack a floor plate, they fail to express *lefty1* in the midline and show bilateral expression of *Nodal, lefty2* and *Pitx2* in the LPM (Meyers and Martin, 1999; Tsukui et al., 1999). The notochord may also have an earlier role as a physical barrier to signal diffusion. The induction of *nodal* expression in the LPM depends on Nodal made in the crown cells of the node. The node-produced Nodal protein appears to travel to the LPM by an internal route (Oki et al., 2007). At this stage, the notochordal plate might act as a physical barrier to Nodal diffusion, although this possibility has not been tested.

The cellular mechanisms that organize the axial mesoderm are not well understood. Convergent extension of the mouse notochordal plate to a strip about 4 cells wide occurs between 0B and 2-somite stages (Yamanaka et al., 2007; Ybot-Gonzalez et al., 2007). In mice that are homozygous for the *Looptail* mutation, which inactivates the core planar cell polarity gene *Vangl2*, the notochord is wider than wild type (Greene et al., 1998; Ybot-Gonzalez et al.,

NIH-PA Author Manuscript

NIH-PA Author Manuscript

NIH-PA Author Manuscript

2007). This wide notochord must be able to serve as an effective midline barrier since, as described above, mutants in the non-canonical Wnt pathway do not show obvious defects in left-right patterning.

Other cellular pathways also appear to be important for generation of the normal axial midline. Integrin signaling is required for the organization of the notochord: mutations in *fibronectin*, a ligand for integrins, and *Paxillin* and *Focal Adhesion Kinase*, components of the signaling complex downstream of integrin receptors, all have a disrupted axial midline (George et al., 1993; Furuta et al., 1995; Hagel et al., 2002). However, the mode of action of integrin signaling in this aspect of morphogenesis has not been defined. Similarly, the axial midline is discontinuous in embryos that lack the FERM domain protein Epb4.1l5, also known as Lulu (Lee et al., 2007). Lulu is important for regulation of the actin cytoskeleton of the primitive streak and neural plate (Lee et al., 2007); future studies will test the role of Lulu, integrin signaling and other cellular pathways in the morphogenesis of the embryonic midline.

Concluding remarks

Like other aspects of vertebrate development, the establishment of left-right asymmetry depends on the integration of transcriptional networks, intercellular signaling pathways, cellular differentiation and tissue morphogenesis. Although generation of the LR pattern is complex, it involves a discrete number of cells and unfolds quickly, which should facilitate dissection of these processes. In addition, the node and midline are on the surface of the mouse embryo and therefore accessible to live imaging in both wild-type and mutant embryos (Yamanaka et al., 2007). As we learn more about the genes required for node specialization and the morphogenetic movements that create the node and axial midline, it should be possible to come to a satisfying understanding of how transcription factors and intercellular signals regulate cilia function and position and the morphogenesis of the node and notochord.

Acknowledgements

We thank Frank Conlon at the University of North Carolina for the generous gift of the Brachyury antibody, and Miquel Tuson and Sarah Goetz for comments on the manuscript. We thank Nina Lampen at the MSKCC Electron Microscopy Core Facility, and Katia Manova and the staff of the MSKCC Molecular Cytology Core Facility, for their expert sample preparation and assistance during SEM and confocal imaging. Our work in this field was supported by NIH grant HD035455.

References

Abdelkhalek HB, Beckers A, Schuster-Gossler K, Pavlova MN, Burkhardt H, Lickert H, Rossant J, Reinhardt R, Schalkwyk LC, Muller I, Herrmann BG, Ceolin M, Rivera-Pomar R, Gossler A. The mouse homeobox gene Not is required for caudal notochord development and affected by the truncate mutation. Genes Dev 2004;18:1725–1736. [PubMed: 15231714]

Amack JD, Wang X, Yost HJ. Two T-box genes play independent and cooperative roles to regulate morphogenesis of ciliated Kupffer's vesicle in zebrafish. Dev Biol 2007;310:196–210. [PubMed: 17765888]

Amack JD, Yost HJ. The T box transcription factor no tail in ciliated cells controls zebrafish left-right asymmetry. Curr Biol 2004;14:685–690. [PubMed: 15084283]

Ang SL, Jin O, Rhinn M, Daigle N, Stevenson L, Rossant J. A targeted mouse Otx2 mutation leads to severe defects in gastrulation and formation of axial mesoderm and to deletion of rostral brain. Development 1996;122:243–252. [PubMed: 8565836]

Ang SL, Rossant J. HNF-3 beta is essential for node and notochord formation in mouse development. Cell 1994;78:561–574. [PubMed: 8069909]

Beckers A, Alten L, Viebahn C, Andre P, Gossler A. The mouse homeobox gene Noto regulates node morphogenesis, notochordal ciliogenesis, and left right patterning. Proc Natl Acad Sci U S A 2007;104:15765–15770. [PubMed: 17884984]

NIH-PA Author Manuscript

NIH-PA Author Manuscript

NIH-PA Author Manuscript

Beddington RS. Induction of a second neural axis by the mouse node. Development 1994;120:613–620. [PubMed: 8162859]

Bellomo D, Lander A, Harragan I, Brown NA. Cell proliferation in mammalian gastrulation: the ventral node and notochord are relatively quiescent. Dev Dyn 1996;205:471–485. [PubMed: 8901057]

Bisgrove BW, Yost HJ. The roles of cilia in developmental disorders and disease. Development 2006;133:4131–4143. [PubMed: 17021045]

Blum M, Andre P, Muders K, Schweickert A, Fischer A, Bitzer E, Bogusch S, Beyer T, van Straaten HW, Viebahn C. Ciliation and gene expression distinguish between node and posterior notochord in the mammalian embryo. Differentiation 2007;75:133–146. [PubMed: 17316383]

Bonnafe E, Touka M, AitLounis A, Baas D, Barras E, Ucla C, Moreau A, Flamant F, Dubruille R, Couble P, Collignon J, Durand B, Reith W. The transcription factor RFX3 directs nodal cilium development and left-right asymmetry specification. Mol Cell Biol 2004;24:4417–4427. [PubMed: 15121860]

Brennan J, Norris DP, Robertson EJ. Nodal activity in the node governs left-right asymmetry. Genes Dev 2002;16:2339–2344. [PubMed: 12231623]

Brody SL, Yan XH, Wuerffel MK, Song SK, Shapiro SD. Ciliogenesis and left-right axis defects in forkhead factor HFH-4-null mice. Am J Respir Cell Mol Biol 2000;23:45–51. [PubMed: 10873152]

Brueckner M. Cilia propel the embryo in the right direction. Am J Med Genet 2001;101:339–344. [PubMed: 11471157]

Cartwright JH, Piro O, Tuval I. Fluid-dynamical basis of the embryonic development of left-right asymmetry in vertebrates. Proc Natl Acad Sci U S A 2004;101:7234–7239. [PubMed: 15118088]

Caspary T, Larkins CE, Anderson KV. The graded response to Sonic Hedgehog depends on cilia architecture. Dev Cell 2007;12:767–778. [PubMed: 17488627]

Chen J, Knowles HJ, Hebert JL, Hackett BP. Mutation of the mouse hepatocyte nuclear factor/forkhead homologue 4 gene results in an absence of cilia and random left-right asymmetry. J Clin Invest 1998;102:1077–1082. [PubMed: 9739041]

Cooper MS, D'Amico LA. A cluster of noninvoluting endocytic cells at the margin of the zebrafish blastoderm marks the site of embryonic shield formation. Dev Biol 1996;180:184–198. [PubMed: 8948584]

Curtin JA, Quint E, Tsipouri V, Arkell RM, Cattanach B, Copp AJ, Henderson DJ, Spurr N, Stanier P, Fisher EM, Nolan PM, Steel KP, Brown SD, Gray IC, Murdoch JN. Mutation of Celsr1 disrupts planar polarity of inner ear hair cells and causes severe neural tube defects in the mouse. Curr Biol 2003;13:1129–1133. [PubMed: 12842012]

Danos MC, Yost HJ. Role of notochord in specification of cardiac left-right orientation in zebrafish and Xenopus. Dev Biol 1996;177:96–103. [PubMed: 8660880]

Davenport JR, Yoder BK. An incredible decade for the primary cilium: a look at a once-forgotten organelle. Am J Physiol Renal Physiol 2005;289:F1159–F1169. [PubMed: 16275743]

Downs KM, Davies T. Staging of gastrulating mouse embryos by morphological landmarks in the dissecting microscope. Development 1993;118:1255–1266. [PubMed: 8269852]

Emery P, Durand B, Mach B, Reith W. RFX proteins, a novel family of DNA binding proteins conserved in the eukaryotic kingdom. Nucleic Acids Res 1996;24:803–807. [PubMed: 8600444]

Essner JJ, Amack JD, Nyholm MK, Harris EB, Yost HJ. Kupffer's vesicle is a ciliated organ of asymmetry in the zebrafish embryo that initiates left-right development of the brain, heart and gut. Development 2005;132:1247–1260. [PubMed: 15716348]

Essner JJ, Vogan KJ, Wagner MK, Tabin CJ, Yost HJ, Brueckner M. Conserved function for embryonic nodal cilia. Nature 2002;418:37–38. [PubMed: 12097899]

Feistel K, Blum M. Three types of cilia including a novel 9+4 axoneme on the notochordal plate of the rabbit embryo. Dev Dyn 2006;235:3348–3358. [PubMed: 17061268]

Frolenkov GI, Belyantseva IA, Friedman TB, Griffith AJ. Genetic insights into the morphogenesis of inner ear hair cells. Nat Rev Genet 2004;5:489–498. [PubMed: 15211351]

Furuta Y, Ilic D, Kanazawa S, Takeda N, Yamamoto T, Aizawa S. Mesodermal defect in late phase of gastrulation by a targeted mutation of focal adhesion kinase. FAK. Oncogene 1995;11:1989–1995.

NIH-PA Author Manuscript

NIH-PA Author Manuscript

NIH-PA Author Manuscript

George EL, Georges-Labouesse EN, Patel-King RS, Rayburn H, Hynes RO. Defects in mesoderm, neural tube and vascular development in mouse embryos lacking fibronectin. Development 1993;119:1079–1091. [PubMed: 8306876]

Greene ND, Gerrelli D, Van Straaten HW, Copp AJ. Abnormalities of floor plate, notochord and somite differentiation in the loop-tail (Lp) mouse: a model of severe neural tube defects. Mech Dev 1998;73:59–72. [PubMed: 9545534]

Hagel M, George EL, Kim A, Tamimi R, Opitz SL, Turner CE, Imamoto A, Thomas SM. The adaptor protein paxillin is essential for normal development in the mouse and is a critical transducer of fibronectin signaling. Mol Cell Biol 2002;22:901–915. [PubMed: 11784865]

Hagiwara H, Ohwada N, Takata K. Cell biology of normal and abnormal ciliogenesis in the ciliated epithelium. Int Rev Cytol 2004;234:101–141. [PubMed: 15066374]

Hamblet NS, Lijam N, Ruiz-Lozano P, Wang J, Yang Y, Luo Z, Mei L, Chien KR, Sussman DJ, Wynshaw-Boris A. Dishevelled 2 is essential for cardiac outflow tract development, somite segmentation and neural tube closure. Development 2002;129:5827–5838. [PubMed: 12421720]

Hirokawa N, Tanaka Y, Okada Y, Takeda S. Nodal flow and the generation of left-right asymmetry. Cell 2006;125:33–45. [PubMed: 16615888]

Huangfu D, Liu A, Rakeman AS, Murcia NS, Niswander L, Anderson KV. Hedgehog signalling in the mouse requires intraflagellar transport proteins. Nature 2003;426:83–87. [PubMed: 14603322]

Hummel KP, Chapman DB. Visceral inversion and associated anomalies in the mouse. J Hered 1959;50:9–13.

Jones C, Roper VC, Foucher I, Qian D, Banizs B, Petit C, Yoder BK, Chen P. Ciliary proteins link basal body polarization to planar cell polarity regulation. Nat Genet 2008;40:69–77. [PubMed: 18066062]

Jurand A. Some aspects of the development of the notochord in mouse embryos. J Embryol Exp Morphol 1974;32:1–33. [PubMed: 4141719]

Kelly KA, Wei Y, Mikawa T. Cell death along the embryo midline regulates left-right sidedness. Dev Dyn 2002;224:238–244. [PubMed: 12112476]

Kelly M, Chen P. Shaping the mammalian auditory sensory organ by the planar cell polarity pathway. Int J Dev Biol 2007;51:535–547. [PubMed: 17891715]

Kinder SJ, Tsang TE, Wakamiya M, Sasaki H, Behringer RR, Nagy A, Tam PP. The organizer of the mouse gastrula is composed of a dynamic population of progenitor cells for the axial mesoderm. Development 2001;128:3623–3634. [PubMed: 11566865]

Kramer-Zucker AG, Olale F, Haycraft CJ, Yoder BK, Schier AF, Drummond IA. Cilia-driven fluid flow in the zebrafish pronephros, brain and Kupffer's vesicle is required for normal organogenesis. Development 2005;132:1907–1921. [PubMed: 15790966]

Krebs LT, Iwai N, Nonaka S, Welsh IC, Lan Y, Jiang R, Saijoh Y, O'Brien TP, Hamada H, Gridley T. Notch signaling regulates left-right asymmetry determination by inducing Nodal expression. Genes Dev 2003;17:1207–1212. [PubMed: 12730124]

Kreiling JA, Williams G, Creton R. Analysis of Kupffer's vesicle in zebrafish embryos using a cave automated virtual environment. Dev Dyn 2007;236:1963–1969. [PubMed: 17503454]

Layton WM Jr. Random determination of a developmental process: reversal of normal visceral asymmetry in the mouse. J Hered 1976;67:336–338. [PubMed: 1021593]

Lee JD, Silva-Gagliardi NF, Tepass U, McGlade CJ, Anderson KV. The FERM protein Epb4.1l5 is required for organization of the neural plate and for the epithelial-mesenchymal transition at the primitive streak of the mouse embryo. Development 2007;134:2007–2016. [PubMed: 17507402]

Levin M. Left-right asymmetry in embryonic development: a comprehensive review. Mech Dev 2005;122:3–25. [PubMed: 15582774]

Liu P, Wakamiya M, Shea MJ, Albrecht U, Behringer RR, Bradley A. Requirement for Wnt3 in vertebrate axis formation. Nat Genet 1999;22:361–365. [PubMed: 10431240]

Lohr JL, Danos MC, Yost HJ. Left-right asymmetry of a nodal-related gene is regulated by dorsoanterior midline structures during Xenopus development. Development 1997;124:1465–1472. [PubMed: 9108363]

McGrath J, Somlo S, Makova S, Tian X, Brueckner M. Two populations of node monocilia initiate left-right asymmetry in the mouse. Cell 2003;114:61–73. [PubMed: 12859898]

NIH-PA Author Manuscript

NIH-PA Author Manuscript

NIH-PA Author Manuscript

Melby AE, Warga RM, Kimmel CB. Specification of cell fates at the dorsal margin of the zebrafish gastrula. Development 1996;122:2225–2237. [PubMed: 8681803]

Meno C, Saijoh Y, Fujii H, Ikeda M, Yokoyama T, Yokoyama M, Toyoda Y, Hamada H. Left-right asymmetric expression of the TGF beta-family member lefty in mouse embryos. Nature 1996;381:151–155. [PubMed: 8610011]

Meno C, Shimono A, Saijoh Y, Yashiro K, Mochida K, Ohishi S, Noji S, Kondoh H, Hamada H. lefty-1 is required for left-right determination as a regulator of lefty-2 and nodal. Cell 1998;94:287–297. [PubMed: 9708731]

Meyers EN, Martin GR. Differences in left-right axis pathways in mouse and chick: functions of FGF8 and SHH. Science 1999;285:403–406. [PubMed: 10411502]

Montcouquiol M, Rachel RA, Lanford PJ, Copeland NG, Jenkins NA, Kelley MW. Identification of Vangl2 and Scrb1 as planar polarity genes in mammals. Nature 2003;423:173–177. [PubMed: 12724779]

Murcia NS, Richards WG, Yoder BK, Mucenski ML, Dunlap JR, Woychik RP. The Oak Ridge Polycystic Kidney (orpk) disease gene is required for left-right axis determination. Development 2000;127:2347–2355. [PubMed: 10804177]

Murdoch JN, Henderson DJ, Doudney K, Gaston-Massuet C, Phillips HM, Paternotte C, Arkell R, Stanier P, Copp AJ. Disruption of scribble (Scrb1) causes severe neural tube defects in the circletail mouse. Hum Mol Genet 2003;12:87–98. [PubMed: 12499390]

Nonaka S, Shiratori H, Saijoh Y, Hamada H. Determination of left-right patterning of the mouse embryo by artificial nodal flow. Nature 2002;418:96–99. [PubMed: 12097914]

Nonaka S, Tanaka Y, Okada Y, Takeda S, Harada A, Kanai Y, Kido M, Hirokawa N. Randomization of left-right asymmetry due to loss of nodal cilia generating leftward flow of extraembryonic fluid in mice lacking KIF3B motor protein. Cell 1998;95:829–837. [PubMed: 9865700]

Nonaka S, Yoshiba S, Watanabe D, Ikeuchi S, Goto T, Marshall WF, Hamada H. De novo formation of left-right asymmetry by posterior tilt of nodal cilia. PLoS Biol 2005;3:e268. [PubMed: 16035921]

Okada Y, Nonaka S, Tanaka Y, Saijoh Y, Hamada H, Hirokawa N. Abnormal nodal flow precedes situs inversus in iv and inv mice. Mol Cell 1999;4:459–468. [PubMed: 10549278]

Okada Y, Takeda S, Tanaka Y, Belmonte JC, Hirokawa N. Mechanism of nodal flow: a conserved symmetry breaking event in left-right axis determination. Cell 2005;121:633–644. [PubMed: 15907475]

Oki S, Hashimoto R, Okui Y, Shen MM, Mekada E, Otani H, Saijoh Y, Hamada H. Sulfated glycosaminoglycans are necessary for Nodal signal transmission from the node to the left lateral plate in the mouse embryo. Development 2007;134:3893–3904. [PubMed: 17913787]

Pennekamp P, Karcher C, Fischer A, Schweickert A, Skryabin B, Horst J, Blum M, Dworniczak B. The ion channel polycystin-2 is required for left-right axis determination in mice. Curr Biol 2002;12:938–943. [PubMed: 12062060]

Placzek M, Tessier-Lavigne M, Yamada T, Jessell T, Dodd J. Mesodermal control of neural cell identity: floor plate induction by the notochord. Science 1990;250:985–988. [PubMed: 2237443]

Poelmann RE. The head-process and the formation of the definitive endoderm in the mouse embryo. Anat Embryol (Berl) 1981;162:41–49. [PubMed: 7283172]

Przemeck GK, Heinzmann U, Beckers J, Hrabe de Angelis M. Node and midline defects are associated with left-right development in Delta1 mutant embryos. Development 2003;130:3–13. [PubMed: 12441287]

Psychoyos D, Stern CD. Fates and migratory routes of primitive streak cells in the chick embryo. Development 1996;122:1523–1534. [PubMed: 8625839]

Rashbass P, Wilson V, Rosen B, Beddington RS. Alterations in gene expression during mesoderm formation and axial patterning in Brachyury (T) embryos. Int J Dev Biol 1994;38:35–44. [PubMed: 7915533]

Raya A, Belmonte JC. Left-right asymmetry in the vertebrate embryo: from early information to higher-level integration. Nat Rev Genet 2006;7:283–293. [PubMed: 16543932]

Raya A, Kawakami Y, Rodriguez-Esteban C, Buscher D, Koth CM, Itoh T, Morita M, Raya RM, Dubova I, Bessa JG, de la Pompa JL, Belmonte JC. Notch activity induces Nodal expression and mediates

NIH-PA Author Manuscript

NIH-PA Author Manuscript

NIH-PA Author Manuscript

the establishment of left-right asymmetry in vertebrate embryos. Genes Dev 2003;17:1213–1218. [PubMed: 12730123]

Roelink H, Augsburger A, Heemskerk J, Korzh V, Norlin S, Ruiz i Altaba A, Tanabe Y, Placzek M, Edlund T, Jessell TM, et al. Floor plate and motor neuron induction by vhh-1, a vertebrate homolog of hedgehog expressed by the notochord. Cell 1994;76:761–775. [PubMed: 8124714]

Satir P, Christensen ST. Overview of structure and function of mammalian cilia. Annu Rev Physiol 2007;69:377–400. [PubMed: 17009929]

Schlueter J, Brand T. Left-right axis development: examples of similar and divergent strategies to generate asymmetric morphogenesis in chick and mouse embryos. Cytogenet Genome Res 2007;117:256–267. [PubMed: 17675867]

Schweickert A, Weber T, Beyer T, Vick P, Bogusch S, Feistel K, Blum M. Cilia-driven leftward flow determines laterality in Xenopus. Curr Biol 2007;17:60–66. [PubMed: 17208188]

Selleck MA, Stern CD. Fate mapping and cell lineage analysis of Hensen's node in the chick embryo. Development 1991;112:615–626. [PubMed: 1794328]

Shawlot W, Behringer RR. Requirement for Lim1 in head-organizer function. Nature 1995;374:425–430. [PubMed: 7700351]

Shiratori H, Hamada H. The left-right axis in the mouse: from origin to morphology. Development 2006;133:2095–2104. [PubMed: 16672339]

Shook DR, Majer C, Keller R. Pattern and morphogenesis of presumptive superficial mesoderm in two closely related species, Xenopus laevis and Xenopus tropicalis. Dev Biol 2004;270:163–185. [PubMed: 15136148]

Sobkowicz HM, Slapnick SM, August BK. The kinocilium of auditory hair cells and evidence for its morphogenetic role during the regeneration of stereocilia and cuticular plates. J Neurocytol 1995;24:633–653. [PubMed: 7500120]

Sulik K, Dehart DB, Iangaki T, Carson JL, Vrablic T, Gesteland K, Schoenwolf GC. Morphogenesis of the murine node and notochordal plate. Dev Dyn 1994;201:260–278. [PubMed: 7881129]

Supp DM, Brueckner M, Kuehn MR, Witte DP, Lowe LA, McGrath J, Corrales J, Potter SS. Targeted deletion of the ATP binding domain of left-right dynein confirms its role in specifying development of left-right asymmetries. Development 1999;126:5495–5504. [PubMed: 10556073]

Swoboda P, Adler HT, Thomas JH. The RFX-type transcription factor DAF-19 regulates sensory neuron cilium formation in C. elegans. Mol Cell 2000;5:411–421. [PubMed: 10882127]

Tabin CJ, Vogan KJ. A two-cilia model for vertebrate left-right axis specification. Genes Dev 2003;17:1–6. [PubMed: 12514094]

Takeda S, Yonekawa Y, Tanaka Y, Okada Y, Nonaka S, Hirokawa N. Left-right asymmetry and kinesin superfamily protein KIF3A: new insights in determination of laterality and mesoderm induction by kif3A−/− mice analysis. J Cell Biol 1999;145:825–836. [PubMed: 10330409]

Takeuchi JK, Lickert H, Bisgrove BW, Sun X, Yamamoto M, Chawengsaksophak K, Hamada H, Yost HJ, Rossant J, Bruneau BG. Baf60c is a nuclear Notch signaling component required for the establishment of left-right asymmetry. Proc Natl Acad Sci U S A 2007;104:846–851. [PubMed: 17210915]

Tanaka Y, Okada Y, Hirokawa N. FGF-induced vesicular release of Sonic hedgehog and retinoic acid in leftward nodal flow is critical for left-right determination. Nature 2005;435:172–177. [PubMed: 15889083]

Torban E, Kor C, Gros P. Van Gogh-like2 (Strabismus) and its role in planar cell polarity and convergent extension in vertebrates. Trends Genet 2004;20:570–577. [PubMed: 15475117]

Tsukui T, Capdevila J, Tamura K, Ruiz-Lozano P, Rodriguez-Esteban C, Yonei-Tamura S, Magallon J, Chandraratna RA, Chien K, Blumberg B, Evans RM, Belmonte JC. Multiple left-right asymmetry defects in Shh(−/−) mutant mice unveil a convergence of the shh and retinoic acid pathways in the control of Lefty-1. Proc Natl Acad Sci U S A 1999;96:11376–11381. [PubMed: 10500184]

Wang Y, Guo N, Nathans J. The role of Frizzled3 and Frizzled6 in neural tube closure and in the planar polarity of inner-ear sensory hair cells. J Neurosci 2006;26:2147–2156. [PubMed: 16495441]

Wang Y, Nathans J. Tissue/planar cell polarity in vertebrates: new insights and new questions. Development 2007;134:647–658. [PubMed: 17259302]

NIH-PA Author Manuscript

NIH-PA Author Manuscript

NIH-PA Author Manuscript

Weinstein DC, Ruiz i Altaba A, Chen WS, Hoodless P, Prezioso VR, Jessell TM, Darnell JE Jr. The winged-helix transcription factor HNF-3 beta is required for notochord development in the mouse embryo. Cell 1994;78:575–588. [PubMed: 8069910]

Yamamoto M, Meno C, Sakai Y, Shiratori H, Mochida K, Ikawa Y, Saijoh Y, Hamada H. The transcription factor FoxH1 (FAST) mediates Nodal signaling during anterior-posterior patterning and node formation in the mouse. Genes Dev 2001;15:1242–1256. [PubMed: 11358868]

Yamamoto M, Mine N, Mochida K, Sakai Y, Saijoh Y, Meno C, Hamada H. Nodal signaling induces the midline barrier by activating Nodal expression in the lateral plate. Development 2003;130:1795–1804. [PubMed: 12642485]

Yamanaka Y, Tamplin OJ, Beckers A, Gossler A, Rossant J. Live imaging and genetic analysis of mouse notochord formation reveals regional morphogenetic mechanisms. Dev Cell 2007;13:884–896. [PubMed: 18061569]

Ybot-Gonzalez P, Savery D, Gerrelli D, Signore M, Mitchell CE, Faux CH, Greene ND, Copp AJ. Convergent extension, planar-cell-polarity signalling and initiation of mouse neural tube closure. Development 2007;134:789–799. [PubMed: 17229766]

Yokoyama T, Copeland NG, Jenkins NA, Montgomery CA, Elder FF, Overbeek PA. Reversal of left-right asymmetry: a situs inversus mutation. Science 1993;260:679–682. [PubMed: 8480178]

Zhang M, Bolfing MF, Knowles HJ, Karnes H, Hackett BP. Foxj1 regulates asymmetric gene expression during left-right axis patterning in mice. Biochem Biophys Res Commun 2004;324:1413–1420. [PubMed: 15504371]

NIH-PA Author Manuscript
NIH-PA Author Manuscript
NIH-PA Author Manuscript

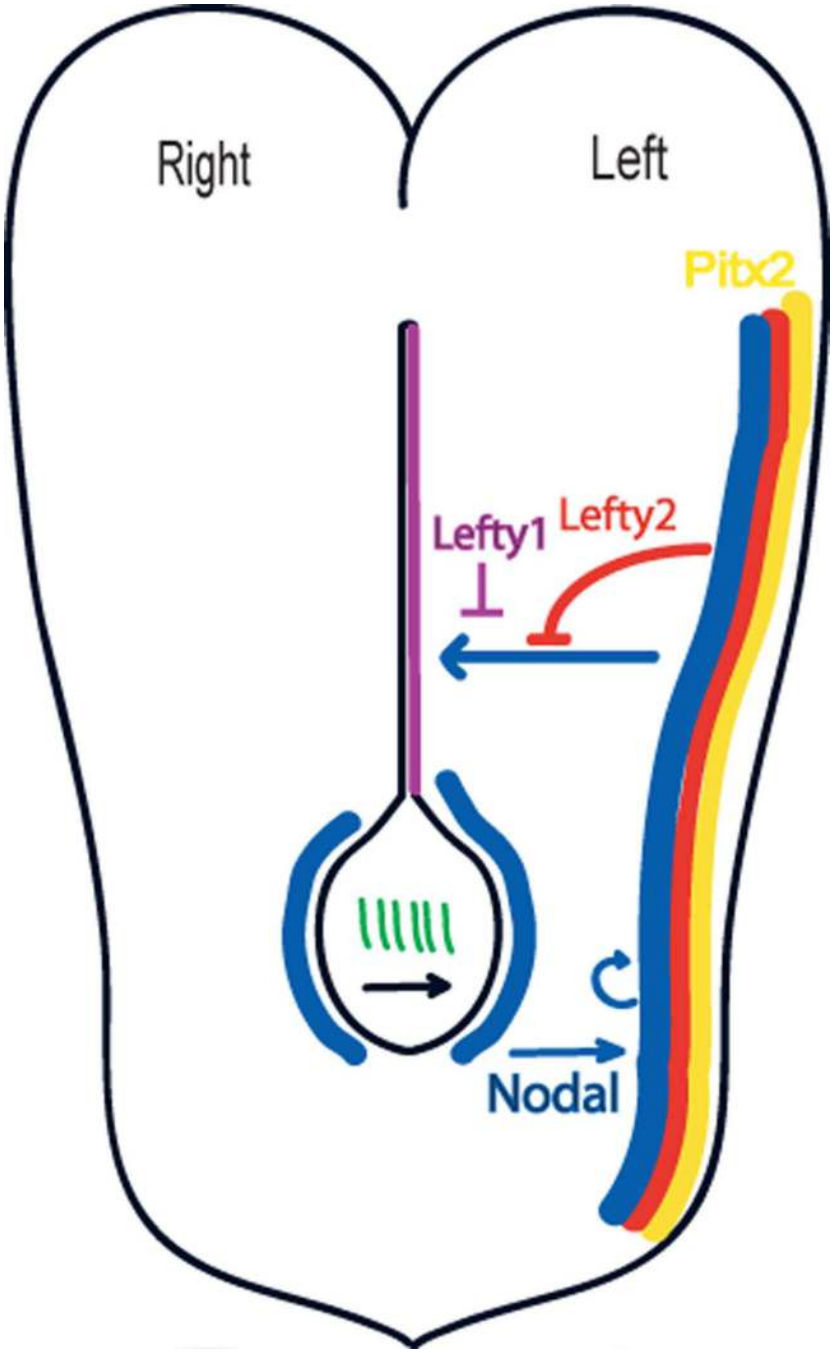

Figure 1.

A simplified schematic of the core left-right signaling pathway in the e8.5 (6 somite) mouse embryo. The embryo is viewed from the ventral side to highlight the ventrally located node. Nodal (blue), a TGFβ family ligand, is expressed around the periphery of the mouse node (outlined in black). Leftward fluid flow across the node requires the correct placement and rotation of nodal cilia (green), and leads to expression of Nodal in the left lateral plate mesoderm (LPM). Nodal signaling in the left LPM induces the expression of upregulates its own expression in a positive feedback loop and also induces expression *lefty2* and *Pitx2*. Lefty2 (red) antagonizes the activity of Nodal and limits its range of activity. Nodal made in the left LPM also activates the expression of *lefty1* (purple) in the left prospective floor plate, dorsal

NIH-PA Author Manuscript

NIH-PA Author Manuscript

NIH-PA Author Manuscript

to the notochord (black line extending anteriorly toward the midline). Lefty1 antagonizes Nodal and prevents the spread of left signaling to the right LPM. The homeodomain transcription factor Pitx2 (yellow) controls later left-sided morphogenetic events. Lack of nodal and Pitx2 expression in the LPM leads to right-sided isomerism in the thorax (e.g. right pulmonary isomerism); bilateral expression of nodal and Pitx2 in the LPM leads to left pulmonary isomerism.

NIH-PA Author Manuscript

NIH-PA Author Manuscript

NIH-PA Author Manuscript

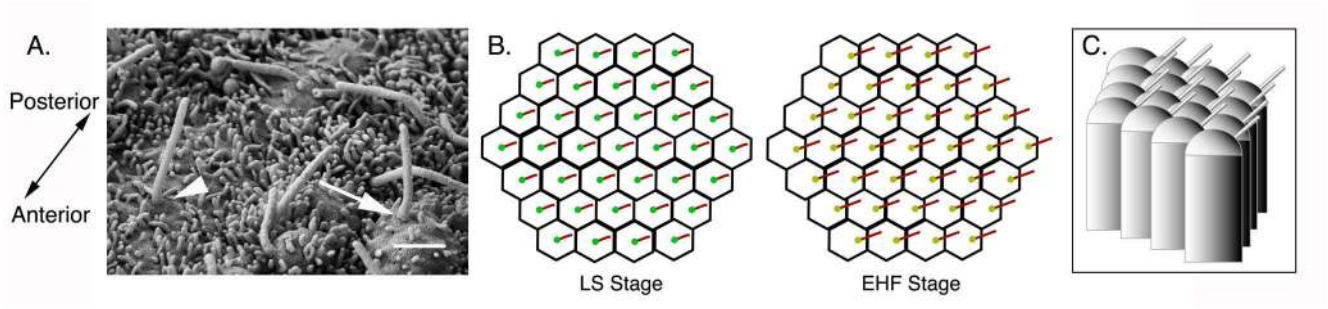

Figure 2.

Cilia position on cells of the node. A. Scanning EM of the node pit at 0B/EHF stage (e8.0). The anterior-posterior axis is labeled. At this stage, some cilia emerge from the center of the cell (arrowhead) and some cilia have shifted to a more posterior position (arrow), while Scale bar = 1 μm. B. Schematics of ventral views of the node pit showing cilia position in cells at LS and EHF stages. Posterior is to the right. At LS stage cilia emerge from the center of each cell; by EHF stage most cilia emerge from the posterior. Nodal flow begins after EHF stage and is well established by LHF stage (e8.25) (Okada et. al., 1999). C. Schematic of lateral view of node pit cells at EHF stage. Posterior is to the right. Cilia emerge from the posterior of each cell; because the apical surface of each cell is domed, the cilia project posteriorly.

NIH-PA Author Manuscript
NIH-PA Author Manuscript
NIH-PA Author Manuscript

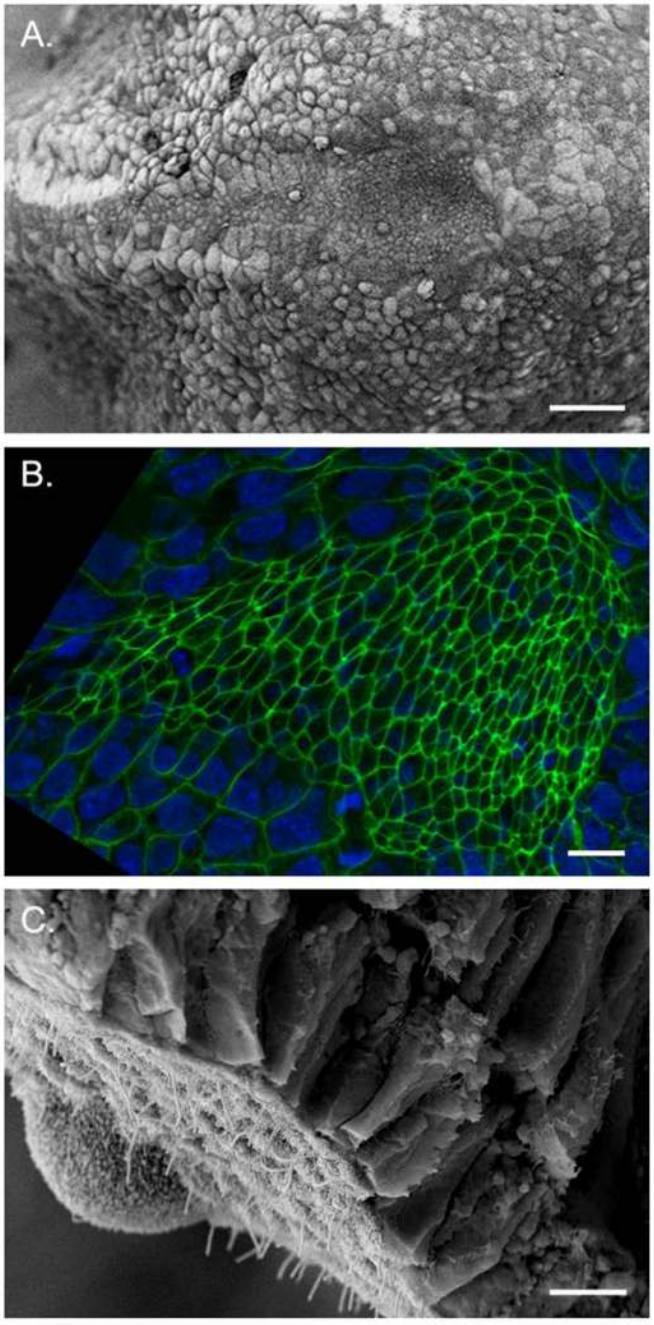

Figure 3.

Morphology of the mature node. A. Scanning electron micrograph (SEM) of EHF (e8.0) stage embryo, ventral view, anterior to the left. The node is visible as a teardrop-shaped pit of cells with small apical surfaces, surrounded by larger squamous crown cells, which are contiguous with the endoderm germ layer. B. Confocal micrograph of an EHF stage embryo showing the ventral node viewed en face, anterior to the left. Phalloidin (green) labels cortical F-actin rings at the apical surface of the polarized node pit cells; DAPI (blue) labels nuclei. Note the small apical surfaces of the cells of the node and axial midline. C. SEM of a LB stage node fractured in the transverse plane, ventral side down. Ciliated, apically constricted ventral node cells are

exposed to the surface, and lie beneath the columnar epithelium of the dorsal node. Scale bars: A. 40μm B. 10μm C. 5μm.

NIH-PA Author Manuscript
NIH-PA Author Manuscript
NIH-PA Author Manuscript

NIH-PA Author Manuscript

NIH-PA Author Manuscript

NIH-PA Author Manuscript

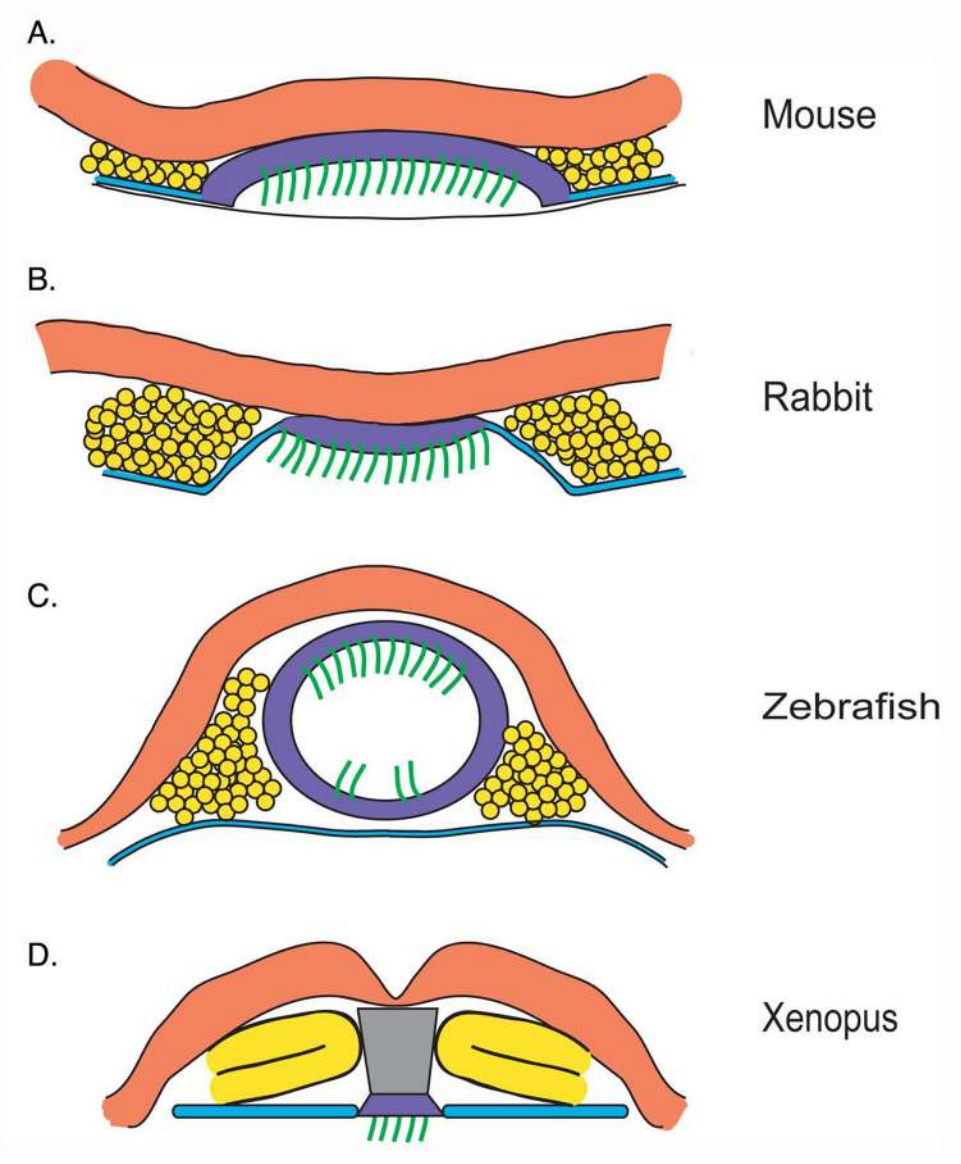

Figure 4.

Comparison of the organs of asymmetry among vertebrate species. Transverse view, dorsal is up. Ectoderm is red, paraxial mesoderm is yellow, endoderm/hypoblast is teal, and the organ of asymmetry is violet, with green cilia. The mouse ventral node and rabbit posterior notochordal plate are positioned beneath the ectoderm and are laterally contiguous with the endoderm/hypoblast. Mesoderm fills the space between the ectoderm and endoderm germ layers lateral to the node. The ventral pit of the mouse node is covered by Reichardt's membrane, creating an enclosed space. The teleost Kupffer's vesicle is an enclosed sphere in zebrafish (shown here) and, in medakafish, a hemisphere; cilia are concentrated on the dorsal anterior surface. The *Xenopus* gastrocoel roof plate is contiguous with the lateral endoderm; cilia project into the gastrocoel cavity. Panels are not size-matched.

NIH-PA Author Manuscript
NIH-PA Author Manuscript
NIH-PA Author Manuscript

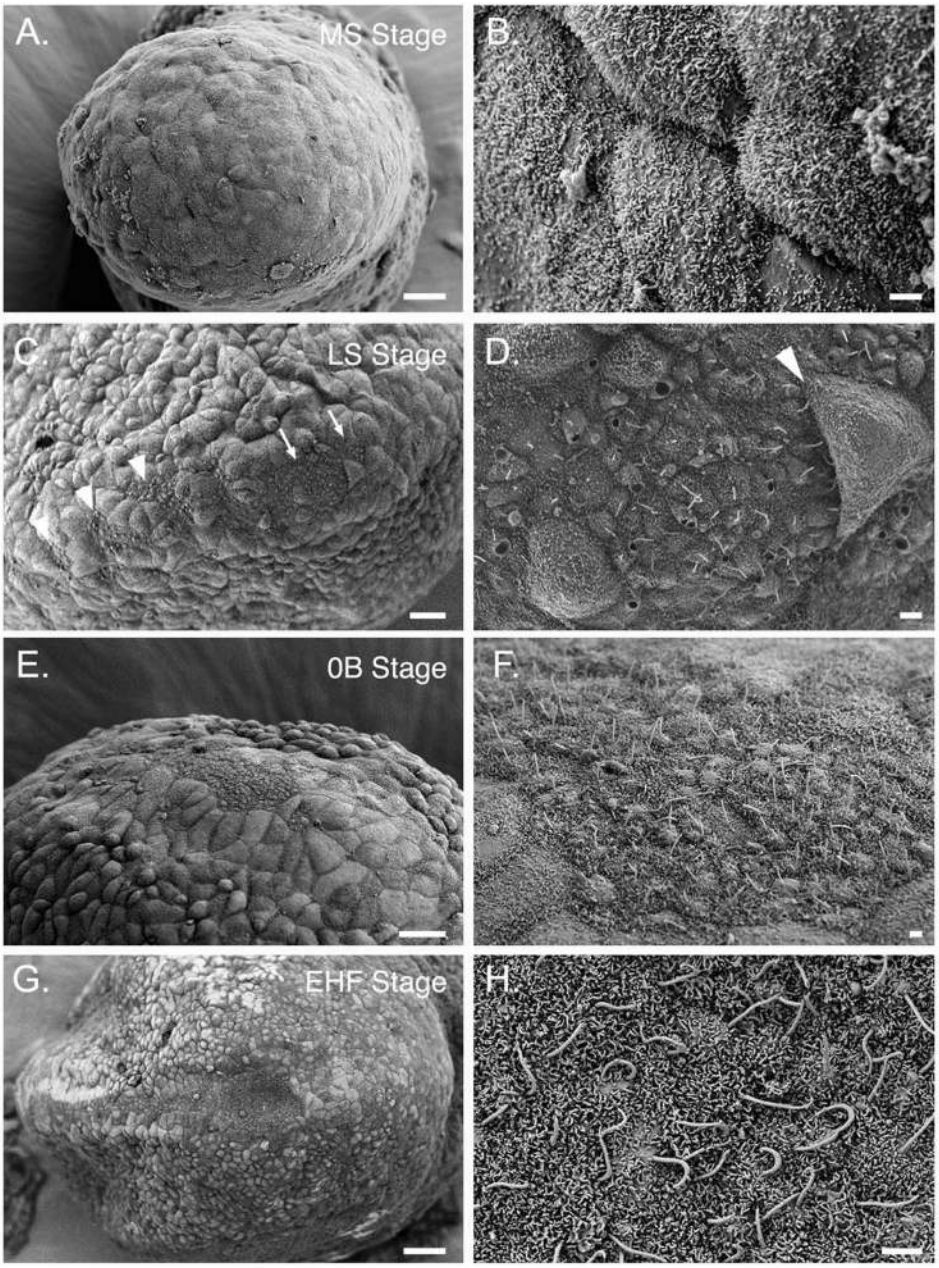

Figure 5.

SEM of the stages of node morphogenesis. All panels show ventral views of the distal tip of the embryo, the position of the node. Anterior is to the left. Staging is according to Downs and Davies (1993). Panels B, D, F and H are higher magnifications of panels A, C, E and G, respectively. (A, B): MS (mid-streak, e7.25) stage. Visceral endoderm distal region of the embryo. (C, D). LS stage (~e7.5). Clusters of cells with small apical surfaces and cilia begin to appear in groups near the presumptive node (arrows, C) and the axial midline (arrowheads, C). Some endoderm cells lie over the node field (arrowhead, D). Most cilia are located in the center of node cells at this stage. (E, F): 0B stage (e7.5–e7.75). The node region is free of overlying endoderm but has not adopted a concave shape. Cilia are longer and continue to project outward. (G, H) EHF stage (~e7.75?). The pit of the node is concave; cilia have

NIH-PA Author Manuscript

NIH-PA Author Manuscript

NIH-PA Author Manuscript

elongated and project posteriorly. The panel in G is a lower magnification view of the embryo shown in Fig. 3A. These images are from embryos in the C3H/HeJ inbred strain. Scale bars: A, C, E, G: 20 μm; B, D, F, H: 2 μm.

NIH-PA Author Manuscript
NIH-PA Author Manuscript
NIH-PA Author Manuscript

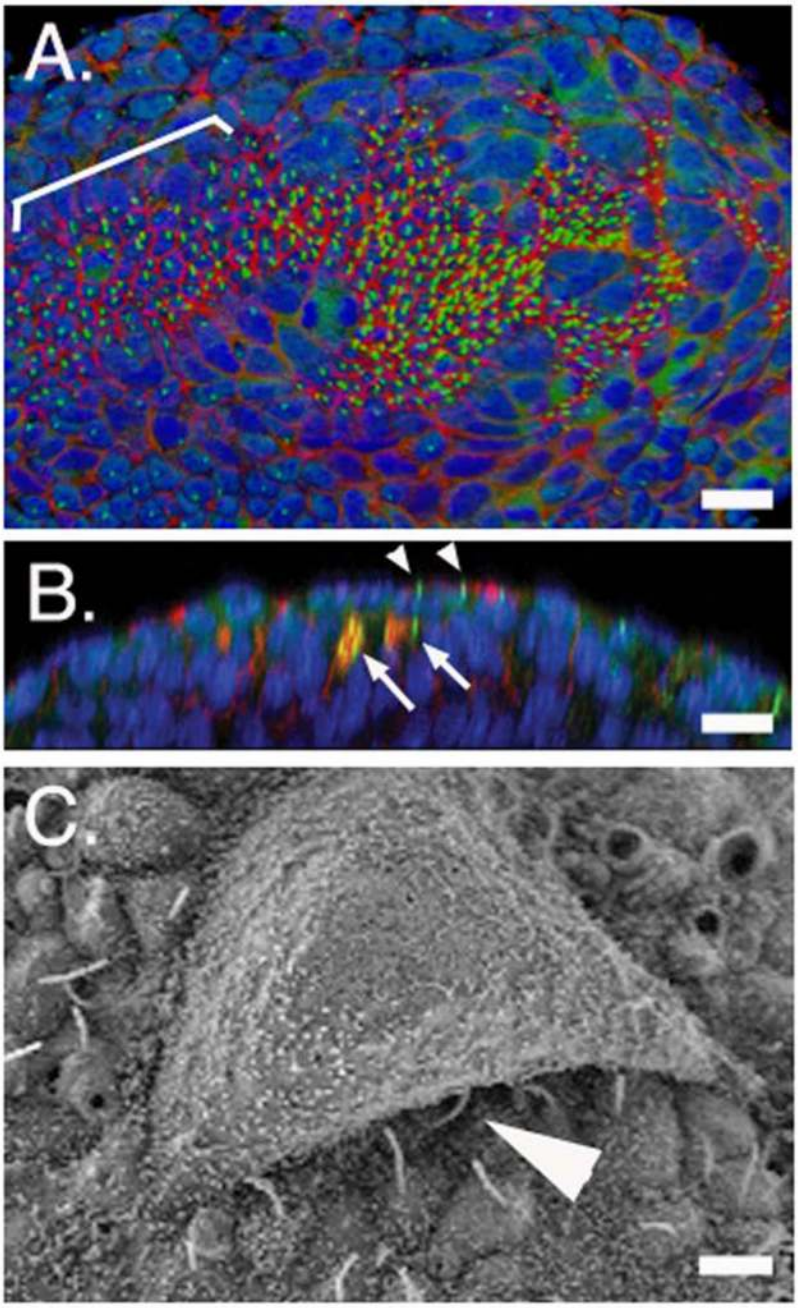

Figure 6.

The intermediate stage of node morphogenesis, when ciliated cells emerge from beneath overlying endoderm. (A, B) Confocal images of embryos labeled with anti-Arl13b (green) to highlight cilia (Caspary et al., 2007), phalloidin (red) to show cell boundaries, and DAPI to label nuclei (blue). A. LS stage embryo, ventral view, anterior to the left; 3D rendering showing scattered clusters of ventral node cells. The notochordal plate (bracket) is visible to the left (anterior). Cilia are mostly located at the center of each cell's apical surface. B. yz-projection of confocal z-stack, LS stage embryo; anterior is up. Cilia (arrows) are visible on some cells still covered by endoderm. Several cilia are visible on cells that have already emerged onto the ventral surface (arrowheads). C. Scanning EM of a LS stage embryo (a higher magnification

of Fig. 5D), showing cilia (arrowhead) visible beneath an overlying endoderm cell. Scale bars: A: 30μm; B: 10 μm; C: 2 μm.

NIH-PA Author Manuscript
NIH-PA Author Manuscript
NIH-PA Author Manuscript

NIH-PA Author Manuscript

NIH-PA Author Manuscript

NIH-PA Author Manuscript

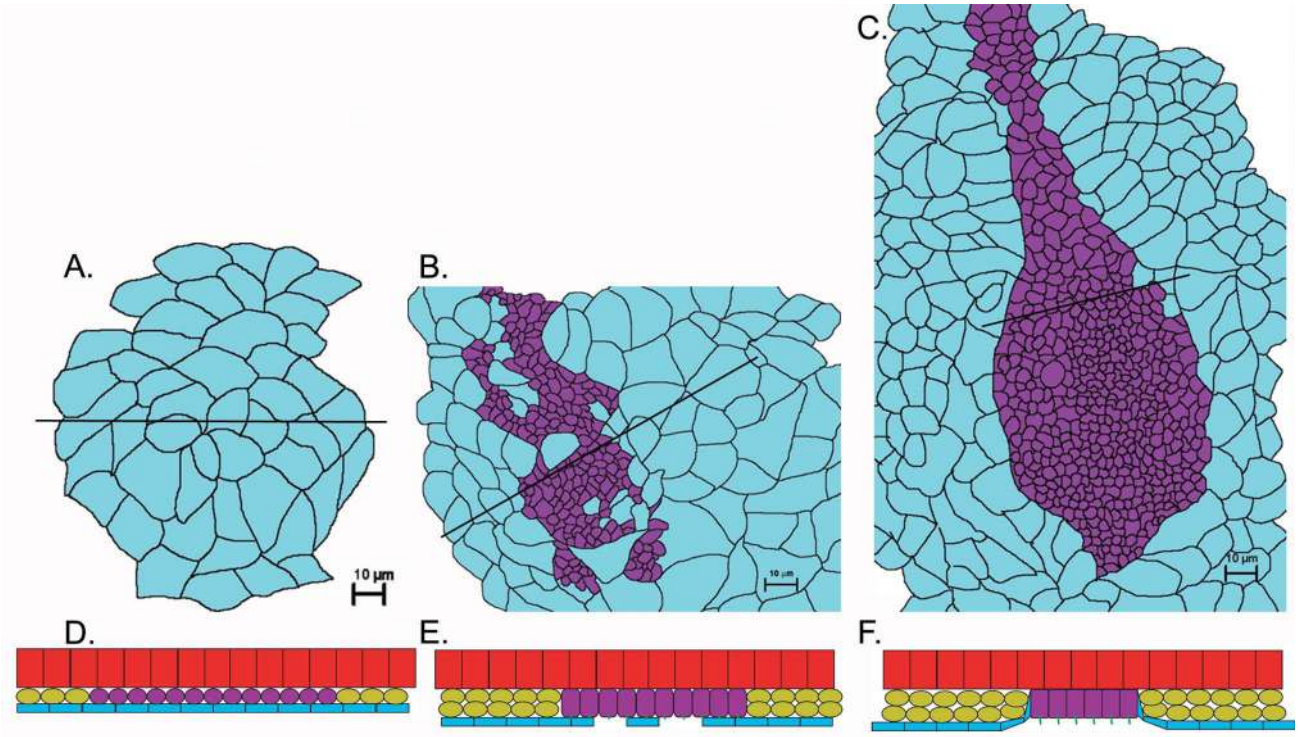

Figure 7.

Steps in node morphogenesis. Camera-lucida-style renderings depict the cell boundaries, traced from SEMs of embryos shown in Fig. 5 A, C and G. A. MS stage. B. LS stage. C. EHF stage. Blue represents endoderm, purple represents ventral node and notochordal plate. Black lines depict approximate plane of section in (D–F). D–F. Cartoons showing a model of node morphogenesis, representing transverse sections through MS, LS and EHF stage nodes showing the arrangement of cell layers. Red = epiblast, purple = ventral node, yellow = paraxial mesoderm, blue = endoderm. (A, D.) Ventral node begins to differentiate prior to emergence onto the ventral surface of the embryo: cells make cilia and begin to epithelialize. (B, E) Emergence occurs gradually during 0B to LB stages, as endoderm is cleared by an unknown process from the distal tip of the embryo. (C, F). Formation of the distinctive pit shape occurs after emergence onto the ventral surface. A–C: anterior up; D–F: epiblast up, endoderm below.

NIH-PA Author Manuscript
NIH-PA Author Manuscript
NIH-PA Author Manuscript

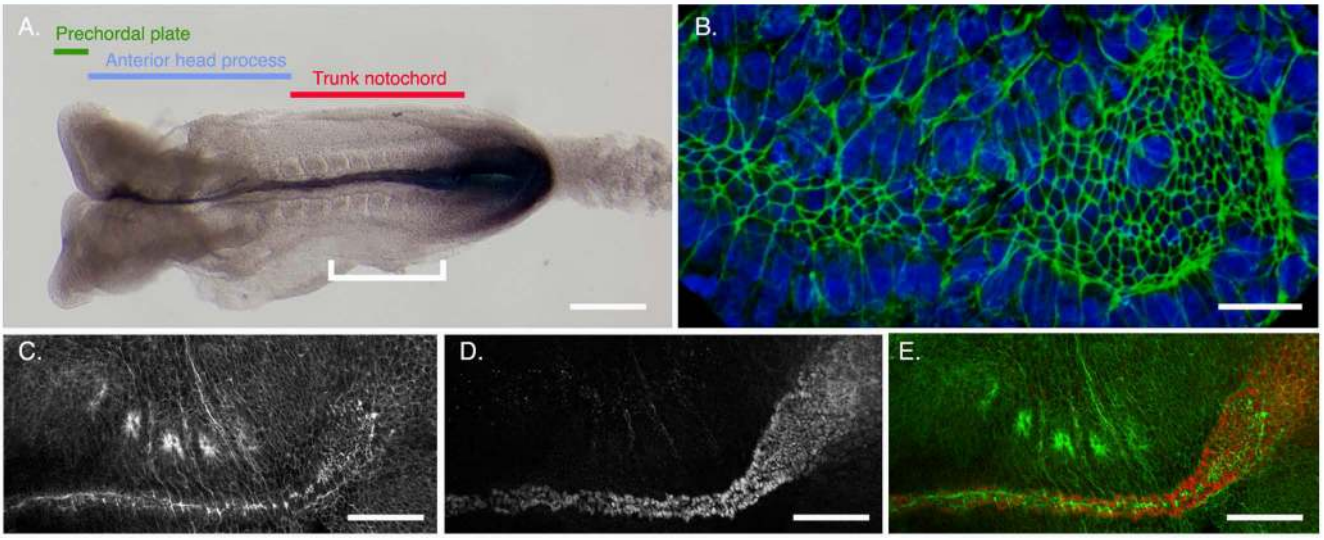

Figure 8.

Morphogenesis of the notochordal plate. A. Regions of the axial midline of e8.5 embryo with 8 somites, dorsal view, anterior to the left, hybridized to reveal expression of *Brachyury (T)*, which is expressed in the primitive streak, node and notochord. Prechordal plate (green) arises from the early gastrula organizer. Anterior head process (blue) arises from the mid-gastrula organizer. Trunk notochord (red) is derived from the node. White bracket is the region shown in (C–F). B. EHF stage embryo, ventral view of the node and axial midline; anterior to the left. Phalloidin (green) labels cell boundaries. Cells with small apical surfaces form a continuous population from the wider node (right) tapering to the notochordal plate (left). The notochordal plate is ~4 cells wide. (C–E). 4-somite embryo, ventral view, anterior to the left. C. Phalloidin staining shows the apically constricted node and notochord cells. The notochord has begun to form a rod along the AP axis; this creates a narrowed line of F-actin staining along the midline. Four somites are visible along the left (upper) flank of the embryo. The curve between the node and notochord is an artifact of the sample preparation. D. Anti-Brachyury immunofluorescence shows nuclei of the notochordal plate and node. E. Merge of (C, D). Scale bars: A: 150 μm; B: 20 μm; C–D: 100 μm.